

Appendix A. Supplementary data

Diagnosing O₃ formation and O₃-NO_x-VOC sensitivity in a heavily polluted megacity of central China: A multi-method systematic evaluation over the warm seasons from 2019 to 2021

Shijie Yu ^a, Hongyu Liu ^a, Hui Wang ^{a*}, Fangcheng Su ^{b,c}, Beibei Wang ^a, Minghao Yuan ^d,
Kunao Song ^a, Zixian Wang ^a, Daoqing Xu ^a, Ruiqin Zhang ^{b,c**}

a. Department of Environmental Engineering, Henan University of Science and Technology, Luoyang 471023, China

b. Institute of Environmental Sciences, Zhengzhou University, Zhengzhou 450001, China

c. School of Ecology and Environment, Zhengzhou University, Zhengzhou 450001, China

d. Environmental Protection Monitoring Center Station of Zhengzhou, Zhengzhou 450007, China

*Correspondence to: H. Wang, Department of Environmental Engineering, Henan University of Science and Technology, Luoyang, Henan, PR China, 471023

**Correspondence to: R. Zhang, Research Institute of Environmental Science, School of Ecology and Environment, Zhengzhou University, Zhengzhou, Henan, PR China, 450001

E-mail address: wanghui79@haust.edu.cn (H. Wang), rqzhang@zzu.edu.cn (R. Zhang)

Figure list

Fig. S1 Locations of the sampling stations in Zhengzhou.

Fig. S2 Four-level nested domains used in the WRF/CMAQ simulations. d01, d02, d03 and d04 have horizontal resolutions of 36, 12, 4 and 1 km, respectively. ZZ: Zhengzhou main city; ZM: Zhongmu; XZ: Xinzheng; XM: Xinmi; DF: Dengfeng; GY: Gongyi; XY: Xingyang.

Fig.S3 Pearson correlation coefficients between pollutants and meteorological factors during the observation period.

Fig. S4 Distribution of typical tracers for different pollutants.

Fig. S5 Diurnal variation distribution of pollutants during different pollution periods.

Fig. S6 The contribution of different sources to O₃ formation.

Fig. S7 Diurnal variation distribution of HOx radicals during the observation period.

Fig. S8 Simulated average formation and loss rates of OH radicals at different pollution levels.

Table list:

Table S1 Parameter table for O₃ simulation calibration in Henan Province

Table S2 Sensitivity distribution of O₃ pollution at different levels.

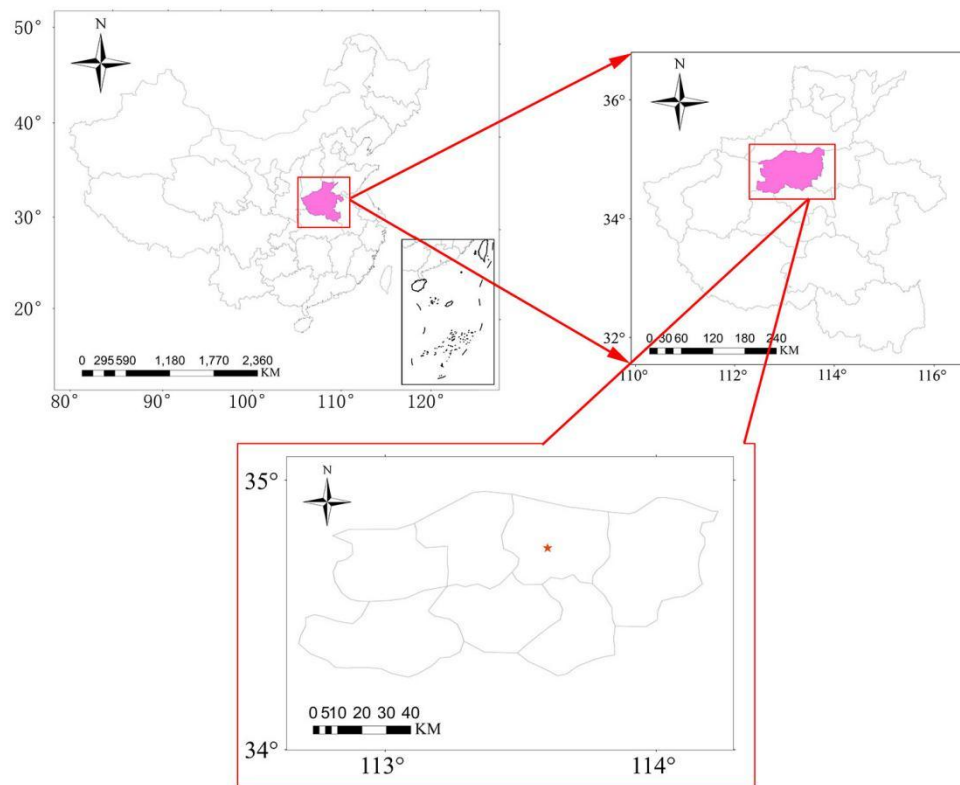


Fig. S1 Locations of the sampling stations in Zhengzhou.

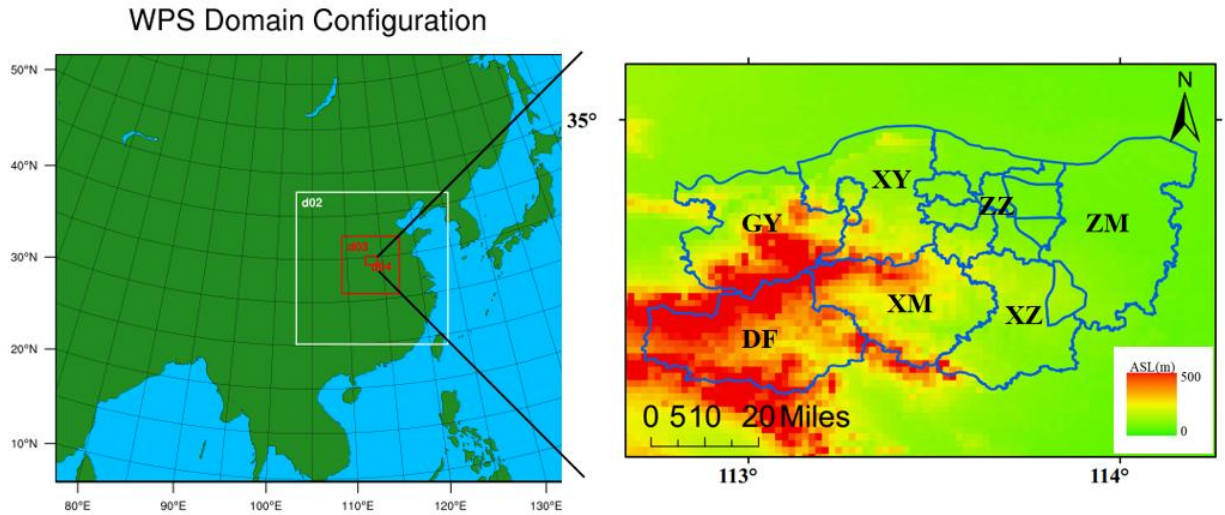
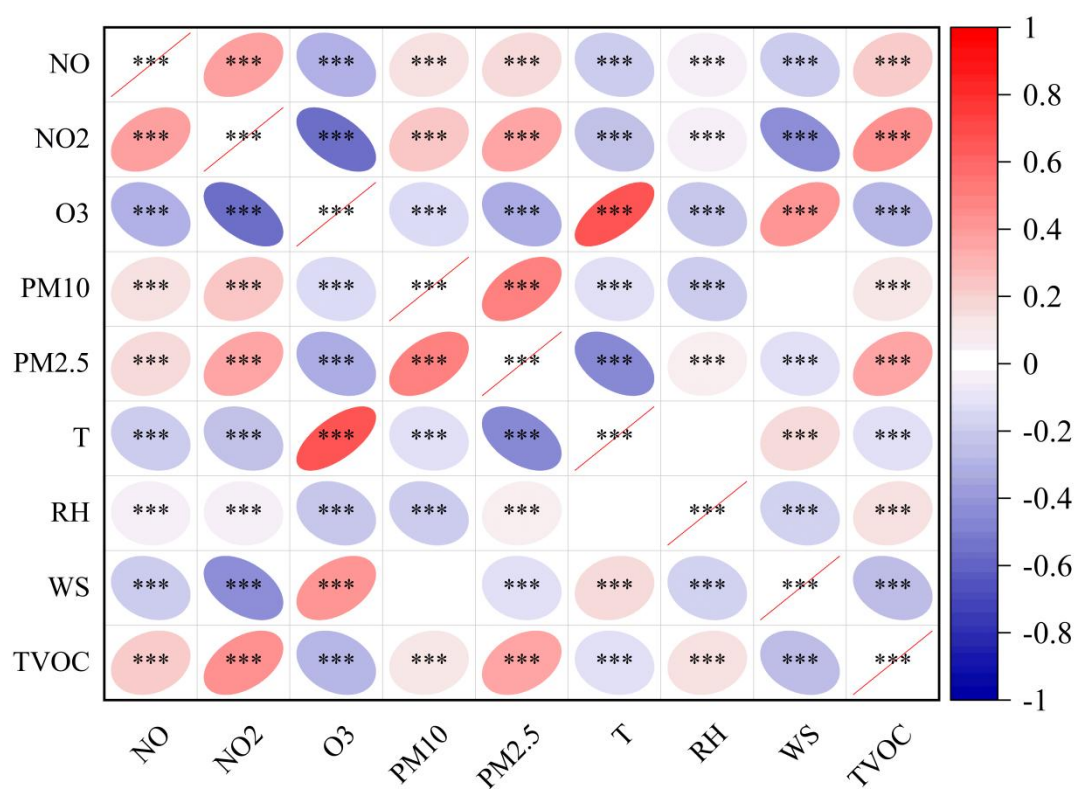


Fig. S2 Four-level nested domains used in the WRF/CMAQ simulations. d01, d02, d03 and d04 have horizontal resolutions of 36, 12, 4 and 1 km, respectively. ZZ: Zhengzhou main city; ZM: Zhongmu; XZ: Xinzheng; XM: Xinmi; DF: Dengfeng; GY: Gongyi; XY: Xingyang.



* $p \leq 0.05$ ** $p \leq 0.01$ *** $p \leq 0.001$

Fig.S3 Pearson correlation coefficients between pollutants and meteorological factors during the observation period.

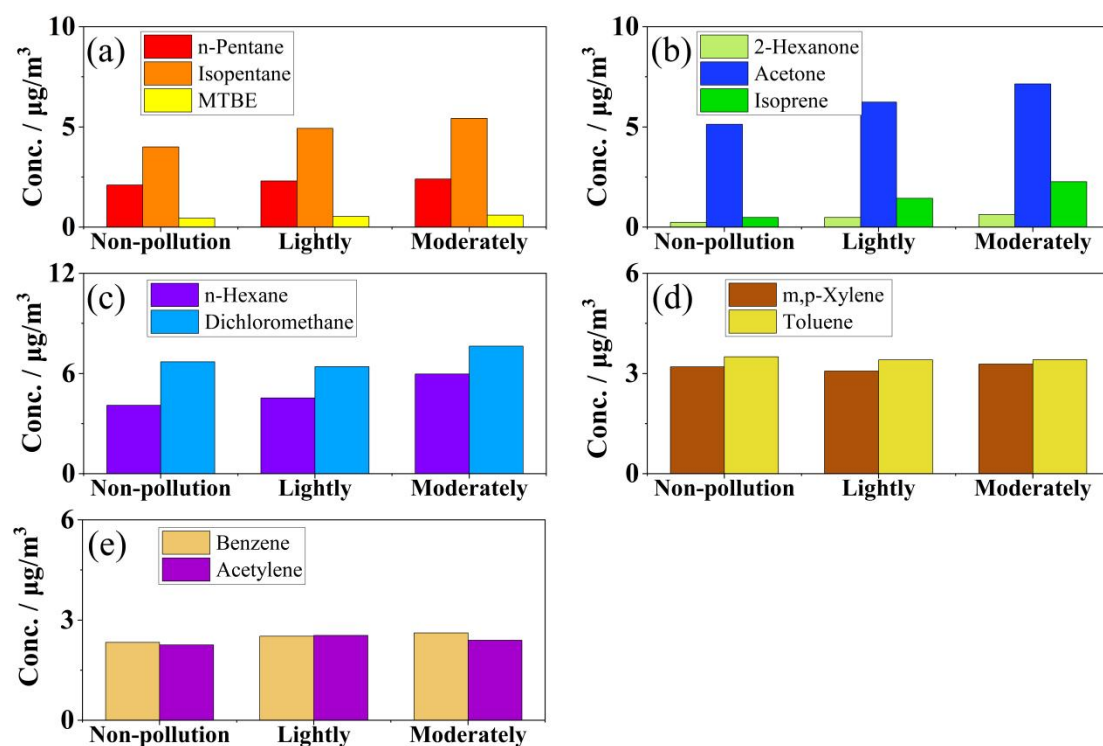


Fig. S4 Distribution of typical tracers for different pollutants.

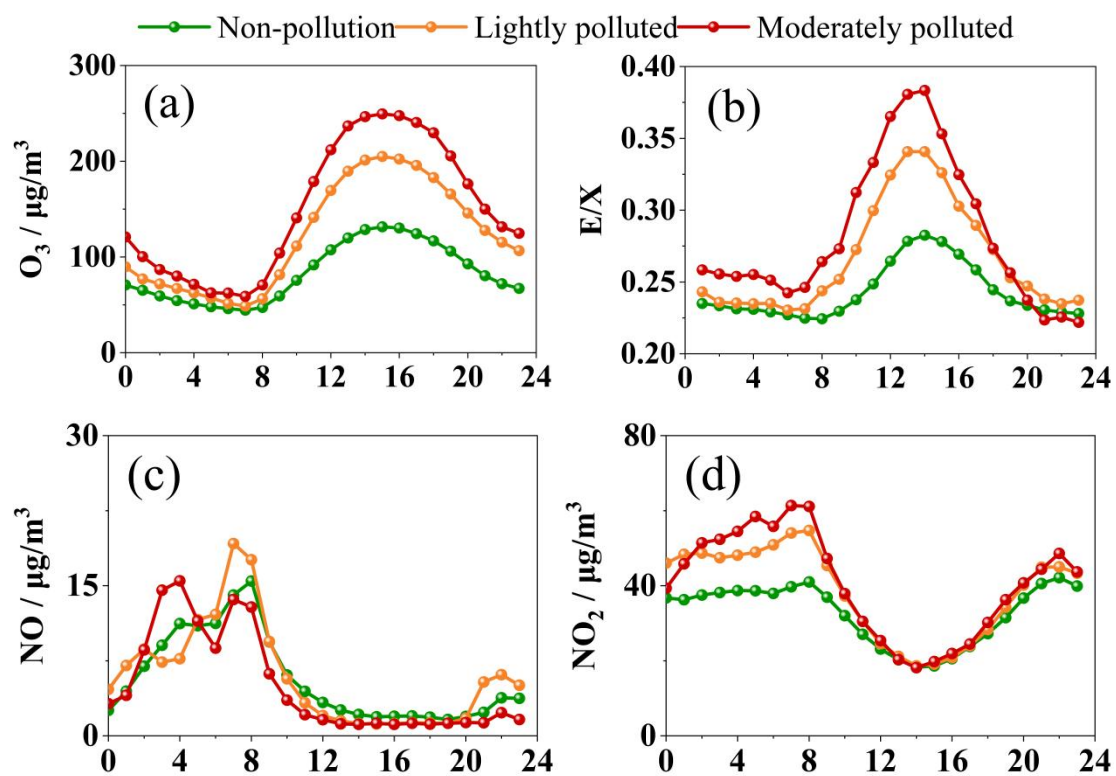


Fig. S5 Diurnal variation distribution of pollutants during different pollution periods.

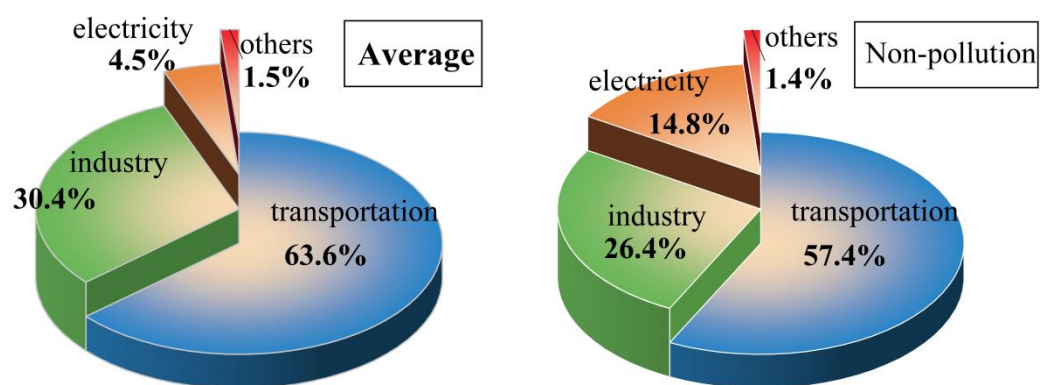


Fig. S6 The contribution of different sources to O₃ formation.

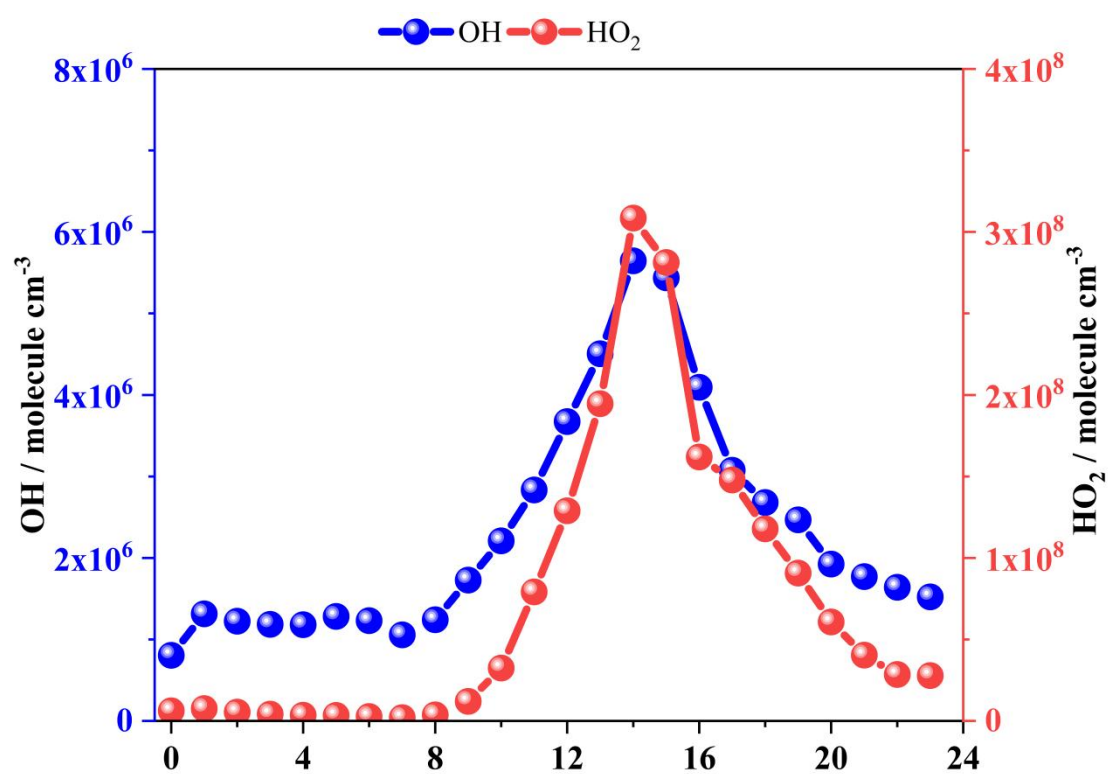


Fig. S7 Diurnal variation distribution of HOx radicals during the observation period.

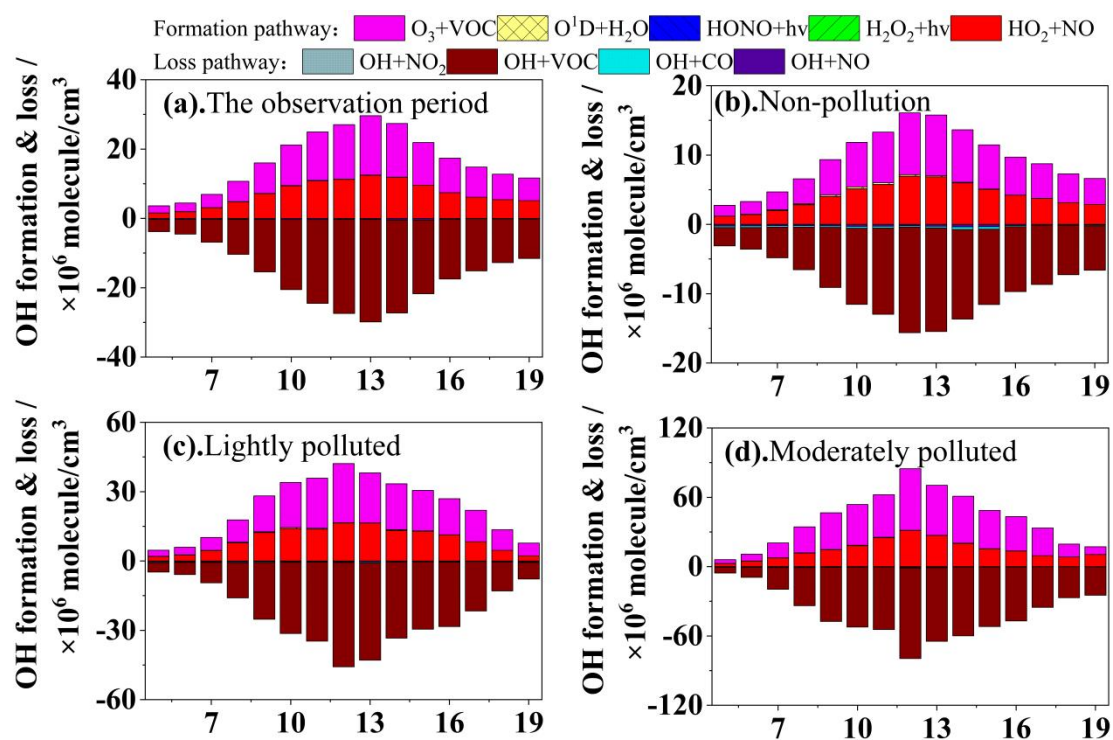


Fig. S8 Simulated average formation and loss rates of OH radicals at different pollution levels.

Table S1 Parameter table for O₃ simulation calibration in Henan Province

	PM _{2.5}	O ₃
Normalized Mean Bias	0.30	-0.21
Normalized Mean Error	0.48	0.25
Mean Fractional Bias	0.21	-0.26
Mean Fractional Error	0.38	0.30
Correlation Coefficient	0.43	0.74

Table S2 Sensitivity distribution of O₃ pollution at different levels.

	VOCs/NO _x	VOCs/NO _x >10
Non-pollution	5.9 ± 7.3	8%
Lightly	7.0 ± 6.6	15%
Moderately	7.3 ± 6.7	18%